



Comparison of short-term breathing rate asymmetry of preeclamptic and normotensive women in labor

Ximena Gonzalez-Reyes¹, Hugo Mendieta-Zerón¹, Eric Alonso Abarca-Castro^{2,a}, Ana Karen Talavera-Peña², Laura Mercedes Santiago-Fuentes^{1,3}, and José Javier Reyes-Lagos^{1,b}

¹ School of Medicine, Autonomous University of the State of Mexico (UAEMéx), Jesús Carranza S/N, 50000 Toluca, State of Mexico, Mexico

² Biological and Health Sciences Division, Autonomous Metropolitan University-Lerma (UAM-L), Avenida de las Garzas 10, 52005 Lerma, State of Mexico, Mexico

³ Biological and Health Sciences Division, Autonomous Metropolitan University-Iztapalapa (UAM-I), San Rafael Atlixco 186, 09340 Mexico City, Iztapalapa, Mexico

Received 29 April 2024 / Accepted 29 August 2024
© The Author(s) 2024

Abstract Breathing rate asymmetry (BRA) refers to the observed disparities in the acceleration and deceleration phases of human respiration. The techniques employed to assess BRA could also be utilized in exploring hypertensive disorders like pre-eclampsia, which is known to cause autonomic cardiorespiratory changes. This study explores features of complexity, including the asymmetry (time irreversibility) of short-term breath-to-breath breathing rate variability among women with severe and moderate pre-eclampsia features compared to those with normal blood pressure. In our study, we retrospectively analyzed continuous respirogram recordings from women in labor, including those diagnosed with severe pre-eclampsia (SP = 22), moderate pre-eclampsia (P = 19), and normotensive control group (C = 35). Using these data, we calculated 5 min of breath-to-breath (BB) time series to measure Porta's index ($P\%$), Guzik's index ($G\%$), and Ehlers' index (E), alongside measures of asymmetrical entropy, including the entropy of acceleration runs (HAR), the entropy of deceleration runs (HDR), and total entropy (H). In addition, Fuzzy Entropy (FuzzEn) and Multiscale Fuzzy Entropy (MFE) over timescales 1–20 were calculated from the BB time series. The nonlinearity was assessed by surrogate analysis. The study's results revealed significant differences in short-term BRA; specifically, mean values of $G\%$ and E were the lowest in SP compared to C and P. Conversely, mean values of the HDR were higher in the SP group than the C. Higher mean values of MFE and a greater percentage of nonlinearity were observed in the SP group as compared to the C group. Our results suggest that women with severe pre-eclampsia may exhibit a higher short-term BRA characterized by a lower contribution of breathing rate decelerations to short-term variability, higher irregularity and nonlinearity of BB time series, and particularly more irregular behavior of decelerations compared to normotensive women. This may indicate a potential modification in the autonomic control of breathing rate and breathing instability.

1 Introduction

Pregnancy brings considerable physiological changes, impacting the cardiovascular and pulmonary systems and body temperature control. While these adjustments are typically normal, specific changes might indicate unusual progression or potential health risks [1]. One such significant condition exclusive to human pregnancy is pre-eclampsia, a critical health issue that poses a substantial threat to the lives of both mothers and newborns. Survivors of pre-eclampsia often face a shortened lifespan and a heightened likelihood of suffering from strokes,

Ximena Gonzalez-Reyes and José Javier Reyes-Lagos contributed equally to this work.

^a e-mail: e.abarca@correo.ler.uam.mx (corresponding author)

^b e-mail: jjreyesl@uaemex.mx (corresponding author)

heart diseases, and diabetes. Additionally, children born from pregnancies affected by pre-eclampsia are at increased risk of being born prematurely, experiencing perinatal death, and suffering from neurodevelopmental issues as well as cardiovascular and metabolic disorders later in life. This complex multisystem disorder is characterized by the sudden onset of high blood pressure occurring after the 20th week of pregnancy, accompanied by at least one additional complication, such as proteinuria, dysfunction of maternal organs, or uteroplacental unit issues [2].

In healthy physiological signals, asymmetry is recognized as a feature of complex nonlinear dynamics. In contrast, pathological states associated with aging or illness often exhibit reduced asymmetry [3]. This loss of balance is evident in the Poincaré plot for heart rate variability (HRV) during normal sinus rhythm, where points are distributed unevenly above and below the identity line, showcasing rapid changes in the interval between heartbeats [4]. Heart rate asymmetry (HRA) has been recently studied in various physiological and pathophysiological contexts, such as in healthy children [5], during head-up tilt tests in healthy men [6], vasovagal syncope in females [7], coronary disease [8], among others. It is a phenomenon of differences between accelerations and decelerations in beat-to-beat heart rate [7].

Previous research from our group has shown that women with pre-eclampsia demonstrate a decreased magnitude of decelerations in heart rate dynamics compared to normotensive women assessed by HRA [9]. This finding suggests that there may be a reduced cardiac parasympathetic response in preeclamptic women during both labor and non-labor periods, in contrast to their normotensive counterparts. Furthermore, it has been observed that women experiencing severe and mild pre-eclampsia during labor may exhibit altered cardiorespiratory coupling compared to normotensive women. In severe pre-eclampsia, disrupted cardiorespiratory coupling may be linked to vagal withdrawal and less intricate cardiorespiratory dynamics. Previous research suggests that variations in vagal activity among preeclamptic groups may indicate a further decline in vagal activity correlating with the severity of the condition [10].

Although crucial, the respiratory or breathing rate is less frequently monitored than other vital signs. Nonetheless, it can act as an early indicator of potential health issues. Recent research has linked variations in breathing patterns to different medical conditions [11]. Similar to HRA, we introduced the concept of Breathing Rate Asymmetry (BRA), which refers to the observed disparities in the acceleration and deceleration of breath-to-breath respiratory rate. Furthermore, breathing rate variability (BRV) reflects the variability in the timing of inhalation or exhalation, influenced by elements such as breath depth and the pauses that follow exhalation and precede inhalation. Airflow patterns determine the breathing rate, and they can be measured with simple devices such as a respiratory belt [10].

Changes in breathing patterns have been demonstrated in women with pre-eclampsia during pregnancy. Pregnant women at high risk with sleep-disordered breathing in mid-gestation exhibited increased arterial stiffness during pregnancy compared to those without such conditions. Sleep-disordered breathing at any point during pregnancy was also associated with a higher risk of pre-eclampsia, with this effect being augmented by hypersomnolence [12]. Wilson et al. (2018) evaluated the frequency of sleep-disordered breathing in women with gestational hypertension and pre-eclampsia compared with body mass index and gestation-matched normotensive pregnant women. They found that more than half of women with a hypertensive disorder of pregnancy meet the clinical criteria for sleep-disordered breathing [13].

According to relevant research, BRV has emerged as a novel measure to study the psychophysiology effects of meditation [14]. Compared to HRV, BRV can provide insights into the short-term effects on the Autonomic Nervous System (ANS) during meditation, whereas HRV is more indicative of long-term effects. In the context of pre-eclampsia, there is limited evidence evaluating BRV and BRA depending on the severity of the preeclamptic condition and assessing its impact on normotensive pregnant women. This suggests a need for more focused studies to understand how these physiological measures can effectively monitor and manage pre-eclampsia in different patient profiles.

Entropy-based methodologies, derived from information theory, are crucial for assessing the complexity and irregularity of physiological signals. Unlike traditional entropy measures, asymmetric entropy evaluates information from monotonic sequences, including constant heart rate accelerations, decelerations, or consecutive RR intervals [15]. Biczuk et al. (2024) explored the use of symmetric entropy in distinguishing atrial fibrillation from sinus rhythm in RR interval time series, showing its potential utility [16]. Furthermore, in time irreversibility analysis, indices such as Porta (P%), Guzik's (G%), and Ehlers (E) have proven effective in identifying time irreversibility, especially in physiological signals [17].

This study explores features of complexity, including the asymmetry (time irreversibility) of short-term breath-to-breath BRV among women with severe and moderate pre-eclampsia symptoms compared to those with normal blood pressure. As a secondary objective, we included the assessment of nonlinearity and irregularity of BRV using entropy measures. This may help to determine the complexity of breathing dynamics in pregnant women, which may differ significantly across varying severities of pre-eclampsia. We hypothesized that in parturient women with pre-eclampsia, BRV and BRA exhibit distinct patterns of asymmetry, irregularity, and nonlinearity when compared to normotensive parturient women, with these differences being more pronounced in severe cases of the condition. These features could noninvasively predict the severity of pre-eclampsia and potentially help monitor the condition more effectively.

2 Methods

2.1 Dataset description

From a previous investigation, a dataset comprising respirograms obtained between 2021 and 2022 at the “Mónica Pretelini Saenz” Maternal-Perinatal Hospital in Toluca de Lerdo, State of Mexico, Mexico was employed to analyze BRA and the irregularity of BRV [10]. Three distinct cohorts of parturient women were examined: the control group (C), comprising 35 normotensive individuals with systolic/diastolic blood pressure of $115.8 \pm 10.7/72.0 \pm 9.2$ mmHg and 39.2 ± 1.2 weeks of pregnancy; the moderate pre-eclampsia group (P), encompassing 19 participants without severe symptoms with systolic/diastolic blood pressure of $140.9 \pm 8.8/90.7 \pm 6.7$ mmHg and 38.6 ± 1.5 weeks of pregnancy; and the severe pre-eclampsia group (SP), consisting of 22 women in labor who exhibited pre-eclampsia meeting severity criteria with systolic/diastolic blood pressure of $152.4 \pm 15.4/101.1 \pm 10.1$ mmHg and 37.5 ± 0.9 weeks of pregnancy. The research committee of the “Mónica Pretelini Saenz” Maternal-Perinatal Hospital granted ethical clearance for the research endeavor (registration number: 2021-03-719), ensuring adherence to specific institutional and broader ethical guidelines during the study’s execution.

The recruitment of participants began by distributing an informed consent form that outlined various aspects relevant to the investigation. This document detailed the study’s objectives, associated risks, potential benefits, and measures to protect data privacy and confidentiality. Participants were provided with comprehensive information to ensure they fully understood these aspects before agreeing to participate in the study. All participants signed the informed consent form.

A compact recording device (Mobi mobile amplifier system, TMSi Systems, The Netherlands) equipped with a respiration sensor affixed to a chest belt was utilized for data collection. The enduring strain assembly of the respiration effort (module V6, Mobi, TMSi Systems, The Netherlands) was deployed to monitor maternal abdominal circumference fluctuations. Twenty minutes of respirograms were captured from participants positioned in a semi-Fowler position, with a sampling frequency of 1000 Hz. All individuals were in their third trimester of pregnancy, and the severity of pre-eclampsia was diagnosed by hospital clinicians based on the criteria set forth by the American College of Obstetricians and Gynecologists (ACOG) [18], corroborated by laboratory assessments including complete blood count, blood chemistry analysis, general urine analysis, and liver function tests.

2.2 Signal pre-processing

Initially, the respirograms from all groups were filtered within a designated frequency band using a band-pass filter with cutoff frequencies ranging from 0.2 to 0.5 Hz [19]. Following this filtering, a peak finder algorithm identified the highest peaks in each respirogram. These peaks were then used to construct the series of consecutive breath-to-breath (BB) intervals. For each respirogram, reliable 5-min segments of these BB interval time series were manually selected. An adaptive filter was applied to these BB interval series to remove artifacts automatically [20]. This additional filtration step was crucial for maintaining the integrity and accuracy of the BB signal analysis. The MATLAB programming language (The MathWorks Inc, Natick, Massachusetts, USA), version R2023, was employed for preprocessing and processing the signals. Subsequently, asymmetrical and entropic features were computed from the BB time series.

2.3 Breathing rate asymmetry (BRA)

This study explored various methods of quantifying asymmetry in BB signals or BRA, ranging from asymmetrical entropy to the indices developed by Porta, Guzik, and Ehlers.

2.3.1 Time-irreversibility indices

Porta’s index, Guzik’s index, and Ehlers’s index were computed from the BB interval time series using the PyBios software [21].

Porta’s index ($P\%$) is calculated by dividing the percentage of negative ΔBB by the total of $\Delta BB \neq 0$. Here ΔBB corresponds to the arithmetic difference of two consecutive BB intervals, $N(\Delta BB -)$ denotes the number of negative ΔBB , and $N(\Delta BB \neq 0)$ indicates the number of all non-zero ΔBB . It measures the contribution of breathing rate accelerations in the short-term [22]:

$$P\% = \frac{N(\Delta BB -)}{N(\Delta BB \neq 0)} \times 100 \quad (1)$$

Guzik's index ($G\%$) is based on the percentage evaluation of the cumulative sum of the squared values of positive ΔBB to the cumulative sum of all squared ΔBB s; it also measures the contribution of breathing rate decelerations in the short-term [23]:

$$G\% = \frac{\sum_{i=0}^{N(\Delta BB^+)} (\Delta BB[i]^+)^2}{\sum_{i=0}^{N(\Delta BB)} (\Delta BB[i])^2} \times 100 \quad (2)$$

Ehlers' index (E) is calculated as the skewness of the probability distribution of the ΔBB expressed as [24]:

$$E = \frac{\sum_{i=0}^{N(\Delta BB)} (\Delta BB[i])^3}{\left(\sum_{i=0}^{N(\Delta BB)} (\Delta BB[i])^2\right)^{3/2}} \quad (3)$$

$G\%$ and $P\%$ are metrics that range from 0 to 100% and are derived from BB time series data. The symmetry assessment in these time series hinges on the median values of $G\%$ and $P\%$. When these median values are close to 50%, it indicates a symmetrical distribution, reflecting an equal balance between accelerations and decelerations in the breathing rate. Values significantly different from 50% suggest the presence of asymmetry or time irreversibility in the breathing pattern. In the context of evaluating other signals like E , symmetry is defined by a benchmark at 0; deviations from this baseline are used as a quantitative measure of the signal's asymmetry [25].

2.3.2 Monotonic runs

We introduce a series of time intervals between breaths, denoted as BB_n , which comprises a sequence $(BB_1, BB_2, \dots, BB_n)$. Further, we explored the sequence of differences between these intervals, labeled $\Delta BB = (\delta_1, \delta_2, \dots, \delta_{n-1})$, where δ_i represents the change from one interval to the next, calculated as $\delta_i = BB_{i+1} - BB_i$. These deltas may exhibit positive, negative, or zero values. Subsequently, we assigned symbolic values to the BB time series changes, categorizing each δ_i as positive, negative, or neutral. This classification allowed us to identify sequences of consistent behavior within the series: a sequence of decelerations, DR_i , consists of consecutive decelerations (positive deltas) bracketed by either an acceleration (negative delta) or no change (zero delta). Conversely, an acceleration sequence, AR_i , includes consecutive accelerations (negative deltas) terminated by either a deceleration (positive delta) or no change. Finally, a neutral sequence, NC_i , is formed by consecutive neutral differences (zero deltas), beginning and ending with either an acceleration or a deceleration. The Fig. 1 shows that the representative BB signal was composed of decelerations: 4 of length 1, 1 of length 2, 1 of length 3; accelerations: 3 of length 1, 1 of length 2, 2 of length 3, and no change: 1 of length 1.

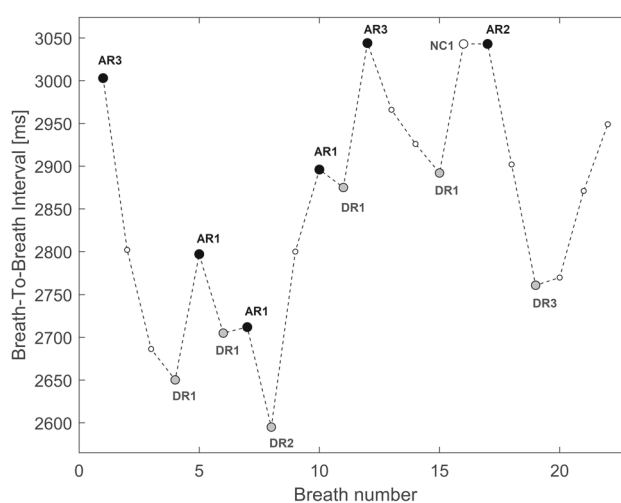


Fig. 1 A representative excerpt from the breath-to-breath (BB) time interval series is depicted based on consecutive runs. These runs are classified into deceleration and acceleration sequences of a specific length denoted as DR_i and AR_i , respectively, while no change sequences are labeled NC_i . A fully shaded grey circle highlights the onset of a deceleration sequence, an acceleration sequence begins with a filled black circle, and the commencement of a neutral sequence is indicated by a fully shaded white circle; the smaller white circles represent the moment where a BB interval starts

In our investigation, we computed the Shannon entropy for each category of run. If we denote $p_{i,k}$ as the probability estimate representing the probability of encountering an interval in the BB recording that corresponds to a specific run type of a particular length:

$$p_{i,k} = \frac{(\text{number of } r_i^k) \times i}{n}, \tag{4}$$

where i represents the run length and k is the run type, which can be AR, DR, NC, the Shannon entropy for this estimator is calculated as follows:

$$H_k = - \sum_{i=1}^{\max(i)k} p_{i,k} \ln p_{i,k} \tag{5}$$

To determine the total entropy of the monotonic runs, we can utilize the following formula:

$$H = HDR + HAR + HNR \tag{6}$$

The MATLAB programming language (The MathWorks Inc, Natick, Massachusetts, USA), version R2023, was employed to compute the asymmetric calculation of entropy based on runs.

2.4 Fuzzy Entropy (FuzzEn)

The algorithm for Fuzzy Entropy, referred to as FuzzEn or FuzzyEn [26] determines the distance measure between pairs of vectors using the following approach:

$$d[X_m(i), X_m(j)] = \max_{0 \leq k \leq m-1} |u(i+k\delta) - u(j+k\delta)|, \text{ where } j > i + \delta \tag{7}$$

FuzzEn utilizes the principles of fuzzy set theory [27], which involves characterizing the degree of similarity between vectors via a fuzzy membership function that relies on calculating the distances between them. The construction of vectors $X_m(i)$ is carried out in a manner akin to that used in Sample Entropy (SampEn), with the key distinction being the subtraction of the average baseline from each vector:

$$X_m(i) = \{u(i+k\delta) - u_0(i) : 0 \leq k \leq m-1\}, \tag{8}$$

where

$$u_0(i) = \frac{1}{m} \sum_{j=0}^{m-1} u(i+j\delta) \tag{9}$$

In the study, we used specific fuzzy membership functions to calculate the indices $B_{ij}^m(r)$ and $A_{ij}^m(r)$, which are defined as:

$$B_{ij}^m(r) = \exp\left(-\frac{d_m^m}{r}\right), \tag{10}$$

and

$$A_{ij}^m(r) = \exp\left(-\frac{d_{m+1}^m}{r}\right), \tag{11}$$

where d is given in Eq. (7) and n is the exponent of the fuzzy membership function. For these computations, the fuzzy membership function implemented in PyBioS by default is $\text{Exp}(-0.6931 \times (d/r)^n)$ [21]. We also define:

$$\phi^m(n, r) = \frac{1}{N - m\delta} \sum_{i=1}^{N-m\delta} B_{ij}^m(r), \tag{12}$$

and

$$\phi^{m+1}(n, r) = \frac{1}{N - m\delta} \sum_{i=1}^{N-m\delta} A_{ij}^{m+1}(r) \quad (13)$$

Thus, FuzzEn is calculated by employing the parameters m , n , r , δ as follows:

$$\text{FuzzEn}(u, m, n, r, \delta) = -\ln\left(\frac{\phi^{m+1}(n, r)}{\phi^m(n, r)}\right) \quad (14)$$

It is important to note that, according to previous studies, Fuzzy Entropy-based algorithms provided better accuracy compared to those based on Sample Entropy (SampEn) for analyzing short-term physiological signals [28]. Consequently, FuzzEn was chosen over SampEn for implementation in this study.

2.5 Multiscale Fuzzy Entropy (MFE)

We calculated the Multiscale Fuzzy Entropy (MFE) from the BB time series using the FuzzEn [29]. These calculations were performed according to the methodology of a previous study [30]. Each element of a coarse-grained time series is calculated according to the equation:

$$u^\tau(j) = \frac{1}{\tau} \sum_{i=(j-1)\tau+1}^{j\tau} u(i), 1 \leq j \leq \frac{N}{\tau} \quad (15)$$

The MFE curve was obtained for 1–20 scales (τ). Each scale defines the window length used for building the coarse-grained time series. Then, we calculate the FuzzEn for each coarse-grained time series of the scale factor τ [31]. The irregularities in the time series for the scale factor τ are quantified by applying FuzzEn for MFE on the coarse-grained time series obtained, with unitary delay ($\delta = 1$), that is:

$$\text{MFE}(u, m, n, r) = \text{FuzzEn}(u^\tau, m, n, r, \delta = 1) \quad (16)$$

2.6 Surrogate analysis

We analyzed surrogate datasets from our BB time series to assess the null hypothesis that these series reflect a stationary linear Gaussian process or simple uncorrelated noise [32]. This assessment produced 200 phase-randomized surrogates for each time series using the Iterative Amplitude-Adjusted Fourier Transform (iAAFT) method, with the iteration count limited to 100 [33]. This procedure preserves the original amplitude distributions. By maintaining the power spectrum, the autocorrelation function of the time series is also conserved. Upon generating the iAAFT surrogates, we computed MFE for scales τ ranging from 1 to 20. This allowed us to scrutinize the linear dynamics hypothesis at each τ for every BB time series of the SP, P, and C groups. A lower MFE in the original series compared to the 5th percentile of MFE values from the surrogates at any given τ led to reject the null hypothesis, indicating nonlinearity at that scale, in line with the approach by Silva et al. [34].

2.7 Statistical analysis

In our statistical analysis, we first examined the data distribution for the normality of C, P, and SP using the Shapiro–Wilk test. For data sets that conformed to a normal distribution, we proceeded with a one-way ANOVA to determine the presence of statistically significant differences among the groups. When ANOVA detected significant differences, post hoc pairwise comparisons were conducted using the Uncorrected Fisher's LSD test. In instances where data did not exhibit normal distribution, a non-parametric Kruskal–Wallis test was employed. Dunn's post hoc test was applied for multiple group comparisons if this test indicated significant differences. Additionally, for MFE, a two-way ANOVA was conducted, followed by a post hoc analysis using the Uncorrected Fisher's LSD test. Statistical significance was set at a p value of less than 0.05. All statistical analyses were performed using GraphPad Prism (GraphPad Software Inc., La Jolla, CA, USA) version 8.02.

3 Results

Figure 2 illustrates significant differences in G% and E among the C, P, and SP groups. Specifically, Fig. 2b shows that G% was significantly lower in the SP ($47.6 \pm 2.3\%$) compared to the C and P groups ($49.3 \pm 2.6\%$ and $50.1 \pm 2.3\%$, respectively). In Fig. 2c, E values also show significant differences; the E mean value was significantly lower in the SP (-1.25 ± 1.32) group compared to the C (0.48 ± 1.19) and P (-0.16 ± 1.16). Additionally, the %P and FuzzEn did not exhibit significant differences.

Figure 3 depicts the MFE values for the BB time series, showing maintained stability across scales 1–20 for the C and P groups. In contrast, individuals with SP exhibit a marked escalation in MFE, beginning at scale 14 and peaking at scale 19. This upturn suggests a considerable increase in signal irregularity. Presented as mean \pm SEM, a statistical significance is noted at scale 19 ($p = 0.0360$) between the C and SP groups (6.09 ± 6.22 vs. 13.67 ± 13.54 , respectively), reflecting the substantial physiological variability associated with severe pre-eclampsia.

Figure 4 illustrates the results of a surrogate analysis, showing the percentage of nonlinear series across scales 1–20 for C, P, and SP. At scale 1, we observed the highest percentages of nonlinearity for all groups: C = 17.14%, P = 13.63%, and SP = 27.27%. Following this, there is a pronounced decrease for the normotensive group, which levels to a minimal entropy across the subsequent scales, suggesting a more predictable, less complex signal. The SP group exhibits a variable but generally declining trend, with intermittent peaks suggesting episodic increases in signal complexity. This pattern emphasizes the increased nonlinearity in the physiological signals of pre-eclamptic subjects, especially at the initial scales.

Figure 5 presents box plots that compare different types of asymmetrical entropies: HDR, HAR, HNO, and H of C, P, and SP. Notably, significant differences were observed in HDR values between the C group and the SP group (Fig. 5a), with the SP group showing a higher median value (C: 1.005 ± 0.0828 vs. SP: 1.056 ± 0.1031 ; $p < 0.05$). This indicates a statistical difference in the HDR measure of asymmetry between these two groups. No other significant differences were apparent among the HAR, HNO, and H entropy measures groups.

In Table 1, we present the mean \pm SD values of the number of acceleration runs (ARi), deceleration runs (DRi), and no-change runs (NCi) observed in the original BB time series. Specifically, the maximum length observed for

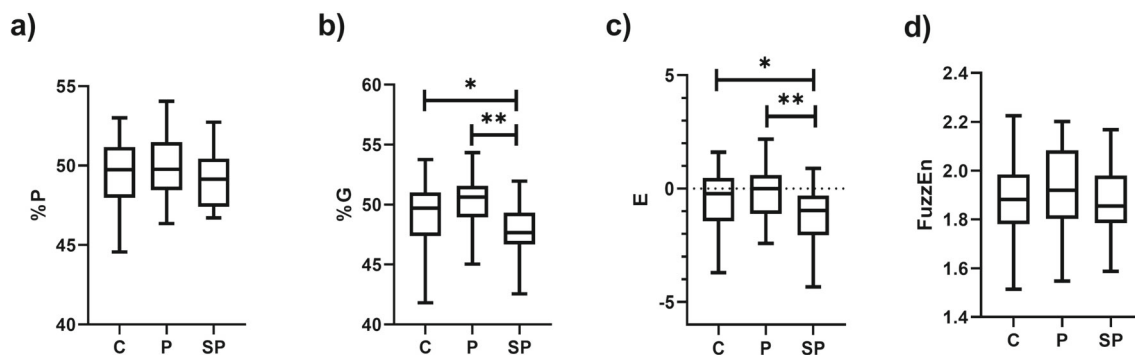


Fig. 2 Box plots of different types of breathing rate asymmetry indices to evaluate the breath-to-breath (BB) signals among healthy normotensive participants (C), moderate pre-eclampsia (P), and pre-eclampsia with severe features (SP) groups. **a** Porta's index (P%), **b** Guzik's Index (G%), **c** Ehlers' index (E) and Fuzzy Entropy (FuzzEn). * $p < 0.05$ between C and SP; ** $p < 0.01$ between P and SP

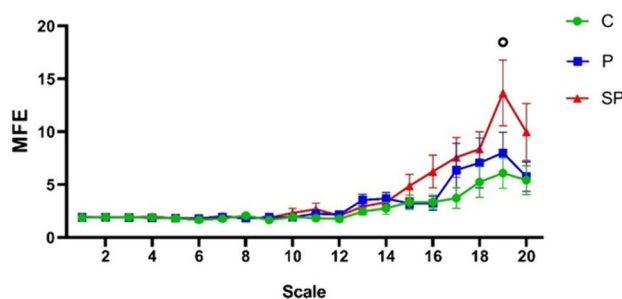


Fig. 3 Multiscale Fuzzy Entropy (MFE) for scales τ ranging from 1 to 20 of breath-to-breath (BB) time series among healthy normotensive participants (C), moderate pre-eclampsia (P), and pre-eclampsia with severe features (SP) groups. Data are shown as mean \pm SEM. ° $p < 0.05$ between C vs SP

Fig. 4 Percentage of nonlinear series (%) of Multiscale Fuzzy Entropy (MFE) across 20 scales. The gray circle represents the control group, the black circle represents the preeclampsia group, and the white circle represents the severe preeclampsia group

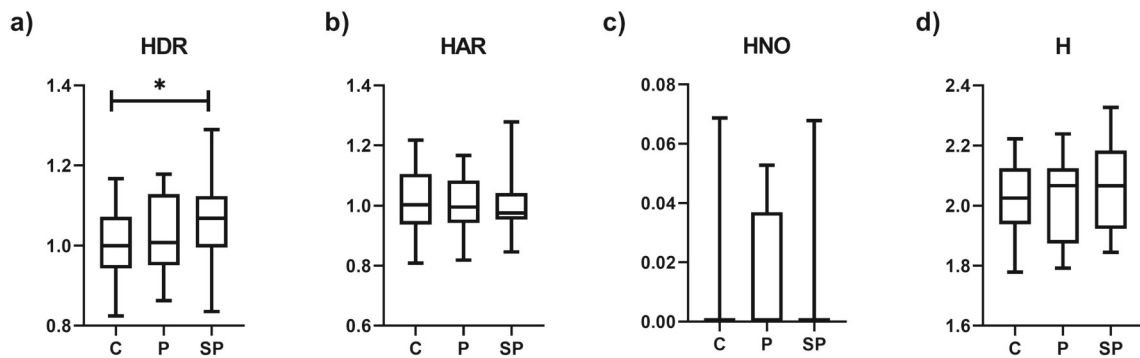
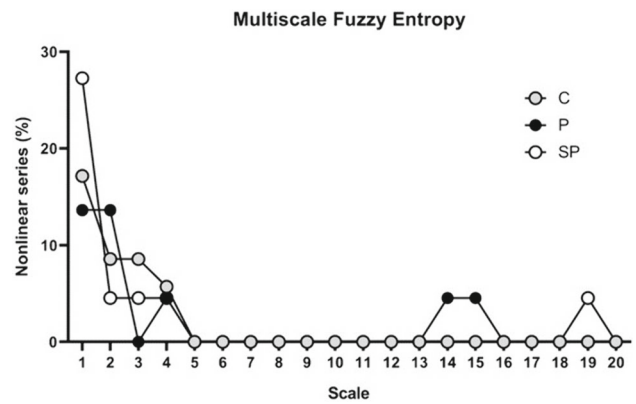


Fig. 5 Box plots of different features of asymmetrical entropy to evaluate the BB time series between normotensive participants (C), moderate pre-eclampsia (P), and pre-eclampsia with severe features (SP) groups. **a** Entropy of deceleration runs (HDR), **b** entropy of acceleration runs (HAR), **c** entropy of no change runs (HNO), and **d** total entropy (H)

Table 1 Run comparison of the number of runs of different lengths in normotensive subjects (C), moderate pre-eclampsia (P), and severe pre-eclampsia (SP)

Runs	C	P	SP
DR1	14.9 ± 5.9	13.4 ± 4.6	13.9 ± 4.6
AR1	14.9 ± 5.1	13.4 ± 3.3	14.1 ± 2.7
NC1	0.1 ± 0.4	0.3 ± 0.4	0.1 ± 0.5
DR2	9.1 ± 3.5	9.2 ± 2.6	8.4 ± 2.4
AR2	8.6 ± 3.7	9.2 ± 3.5	9.0 ± 3.1
NC2	0.0 ± 0.0	0.0 ± 0.0	0.0 ± 0.0
DR3	3.9 ± 1.8	3.7 ± 1.6	3.9 ± 1.7
AR3	4.0 ± 1.8	3.6 ± 1.9	3.8 ± 1.8
NC3	0.0 ± 0.0	0.0 ± 0.0	0.0 ± 0.0
DR4	1.6 ± 1.1	1.4 ± 1.1	2.0 ± 1.2
AR4	1.7 ± 1.1	1.4 ± 1.3	1.5 ± 1.1
NC4	0.0 ± 0.0	0.0 ± 0.0	0.0 ± 0.0
DR5	0.5 ± 0.8	0.6 ± 0.8	0.4 ± 0.6
AR5	0.4 ± 0.6	0.5 ± 0.8	0.3 ± 0.6
NC5	0.0 ± 0.0	0.0 ± 0.0	0.0 ± 0.0
DR6	0.1 ± 0.3	0.1 ± 0.3	0.1 ± 0.3
AR6	0.2 ± 0.5	0.1 ± 0.3	0.1 ± 0.5
NC6	0.0 ± 0.0	0.0 ± 0.0	0.0 ± 0.0

both acceleration and deceleration runs was 6, whereas for no-change runs, only a length of 1 was observed. No significant differences were observed among ARi, DRi, and NCi for the studied groups.

4 Discussion

This study explored features of complexity, including the asymmetry (time irreversibility) of short-term breath-to-breath variability in breathing rate among women with severe and moderate pre-eclampsia symptoms compared to those with normal blood pressure. Our findings can be summarized into three key points: (1) women with severe pre-eclampsia may exhibit higher short-term BRA or time irreversibility, characterized by a reduced contribution of breathing rate decelerations compared to normotensive women and those with moderate pre-eclampsia; (2) women with severe pre-eclampsia showed higher irregularity in BRV compared to normotensive women, particularly a more irregular behavior of decelerations of breathing rate; (3) similarly, women with severe pre-eclampsia demonstrated greater nonlinearity in their breathing pattern time series compared to normotensive women. These findings suggest a potential alteration in the autonomic control of breathing rate in severe pre-eclampsia associated with a more complex dynamics of breathing rate.

Concerning our first key finding, the results of our study highlighted significant deviations in BRA among women with severe pre-eclampsia. Specifically, these women exhibited significant differences from the median value of 50% and 0 in indices such as $G\%$ and E . These decreases in $G\%$ and E within the severe pre-eclampsia group indicate a deviation from the ideal symmetry of breathing patterns. Typically, median values close to 50% signify a symmetrical distribution, reflecting an equal balance between accelerations and decelerations in the breathing rate. However, values substantially different from 50% or 0—as observed in severe pre-eclampsia—indicate the presence of asymmetry or time irreversibility. This physiological phenomenon may indicate a disrupted autonomic control or breathing instability, with breathing rate decelerations less prominent compared to normotensive women or those with moderate pre-eclampsia. Such changes are likely driven by complex interactions involving the autonomic nervous system, cardiovascular adjustments, and systemic inflammation characteristic of this condition [35]. These findings align with previous results from our research group, where it was found that severe pre-eclampsia could be associated with a decrease in parasympathetic activity or an increase in sympathetic activity [9] and a reduction in cardiorespiratory coupling [10]. According to Karmakar et al., the manifestation of asymmetry can be an expected phenomenon of a healthy physiologic system, but it can be increased or decreased in pathologic conditions [36].

Furthermore, in our second key finding, the analysis of entropy measures provided additional insights into the irregularity of respiratory dynamics in pregnant women with severe pre-eclampsia. Interestingly, by using the MFE approach, it is possible to discriminate between the women with SP and those without the disease (Fig. 3, $p < 0.05$). The distinct patterns observed across different scales and the significant differences in the MSE of women with severe pre-eclampsia suggest higher irregularity in breathing rate fluctuations in the SP group, which may reflect underlying physiological perturbations associated with pre-eclampsia.

Reflecting on the heightened irregularity revealed through MFE in our study, there appears to be a consistency with Anderson's research, which identified a significant elevation in the BRV alongside other respiratory parameters in women with raised systolic blood pressure [37]. This increase in BRV is particularly noteworthy, as it aligns with the irregular breathing patterns—indicated by larger MFE values—that we observed in women suffering from severe pre-eclampsia. While the causal linkage between periodic breathing and chronic hypertension is still under investigation, the suggested autonomic dysregulation involving heightened sympathetic or reduced parasympathetic activity might well explain the respiratory irregularities, including the variability in respiratory rate that the MFE analysis demonstrated in the SP group.

Finally, the graphical representation in Fig. 4 suggests that the BRV among normotensive parturient women and those with moderate pre-eclampsia exhibits a minimal contribution of nonlinear components. We thus hypothesize that increased complexity in the time series of BB intervals in severe pre-eclampsia might represent an adverse condition. In contrast, the BB patterns in normotensive women appear more regular or simpler, characterized by complexity features such as lower asymmetry (time irreversibility), decreased irregularity, and reduced nonlinearity. The surrogate analysis undertaken in our investigation reinforces our findings by highlighting the presence of nonlinearity in the BRV of women with pre-eclampsia.

However, we must consider the limitations of our work. The relatively small cohort size and the study's confinement to a single center may affect how widely our results can be applied. Moreover, other cardiovascular risk factors should be considered in the study for all three groups, as they could have impacted our results. For instance, significant differences were observed in mean heart rate between the control group (78.2 ± 11.7 BPM) and severe pre-eclampsia (94.5 ± 14.4 BPM) ($p < 0.0001$) and between severe pre-eclampsia and pre-eclampsia (81.2 ± 16.9 BPM) ($p < 0.01$). This is consistent with what has been reported in the literature regarding the interaction or dependency between the cardiac and respiratory systems [38, 39]. No significant differences were observed in weight between the groups. BMI differences were significant between the control group (28.7 ± 4.9 kg/m²) and

the pre-eclampsia group ($31.8 \pm 4.9 \text{ kg/m}^2$) ($p < 0.05$). However, we consider that the changes are mainly due to the pre-eclamptic condition.

It is important to note that, to the best of our knowledge, this is the first study to report short-term BRA measurements in pregnant women with and without pre-eclampsia. Consequently, finding comparable results from another research where BRA has been used was challenging. Previous studies have primarily employed BRV and HRA measurements in physiological and pathological scenarios. For example, evidence suggests that breathing instability, as indicated by higher BRV, is observed in obstructive sleep apnea compared to controls during wakefulness [40]. We speculate that increased breathing instability could be associated with greater asymmetry during pre-eclampsia. Notably, recent studies indicate potential associations between respiratory rate and HRA [41].

Van den Bosh's research indicates that the variability in respiratory patterns over time could serve as an indicator for identifying individuals at risk of developing pulmonary complications [42]. The complexity of BRV is not yet completely understood. Assessing the variability in a singular respiratory metric, such as the breathing rate, might not encapsulate the full scope of variability in the respiratory system. Conditions such as Chronic Obstructive Pulmonary Disease, restrictive lung diseases, chronic pulmonary disorders originating in infancy, non-rapid eye movement sleep, and cognitively demanding tasks are known to reduce the variability in respiratory patterns. In contrast, this variability tends to increase among elderly individuals when they are engaged in complex numerical tasks, in hypoxic conditions, and among patients with asthma, hypertension, or anxiety disorders. Comprehensive research is still needed to fully grasp the implications of BRV in the domains of critical care.

5 Conclusion and outlook

This investigation has cast light on the features of complexity in short-term breathing rate asymmetry (BRA) and its variability (BRV) among women with varying severities of pre-eclampsia compared to normotensive pregnant women. The study showed that severe pre-eclampsia is associated with a higher degree of short-term BRA, underpinned by a distinctive reduction in breathing rate decelerations and an overall higher irregularity and nonlinearity in the breath-to-breath (BB) time series. Thus, the dynamics of short-term BB breathing rate variability appear to be more complex in severe pre-eclampsia than in the more regular or simpler patterns observed in normotensive women or those with moderate pre-eclampsia. This suggests that the autonomic control of respiratory rate may be disrupted in severe pre-eclampsia, potentially leading to more complex breathing dynamics.

Our data demonstrated significant asymmetry in breathing patterns, particularly in the severe pre-eclampsia group, as reflected by significant deviations from median values in indices measuring time irreversibility. The implications of these findings are relevant, suggesting alterations in autonomic function and potentially contributing to the systemic pathophysiological changes characteristic of severe pre-eclampsia. Overall, the study underscores the potential of BRV and BRA as noninvasive markers for assessing the severity of pre-eclampsia and for monitoring the condition in expectant mothers. With further research, these measures could prove to be invaluable tools in obstetrics, potentially offering a window into the intricate interplay of physiological systems during pregnancy and their response to pathological states.

Acknowledgements The authors thank the study participants and the Mónica Pretelini Hospital staff. We also thank Rosselin Gabriela Ceballos-Juárez and Elias Yojairi Pichardo-Carmona for their valuable support during data collection.

Author contributions

XG-R conducted formal analysis, investigation, prepared the original draft, validated the study findings, and contributed to visualization. HM-Z provided supervision and managed project administration. EAA-C and AKT-P both handled supervision and were involved in writing, review, and editing of the manuscript. LMS-F also contributed to supervision and manuscript editing. JJR-L conceptualized the study, prepared the original draft, and was involved in writing, review, editing, and providing resources. Each author's efforts were integral to the comprehensive exploration and documentation of the study.

Funding Open access funding provided by Universidad Autonoma Metropolitana (BIDIUAM).

Data availability The authors declare that the data supporting this study's findings (BB time series and clinical data such as heart rate, weight, and body mass index) are available in the institutional repository of UAM-L. The dataset is freely available at <http://hdl.handle.net/20.500.12222/429> or <https://xogi.ler.uam.mx/items/09cf5a77-4fb0-48fb-a65c-fea2dcb854fd>.

Declarations

Conflict of interest The authors declare that no competing interests exist.

Open Access This article is licensed under a Creative Commons Attribution 4.0 International License, which permits use, sharing, adaptation, distribution and reproduction in any medium or format, as long as you give appropriate credit to the original author(s) and the source, provide a link to the Creative Commons licence, and indicate if changes were made. The images or other third party material in this article are included in the article's Creative Commons licence, unless indicated otherwise in a credit line to the material. If material is not included in the article's Creative Commons licence and your intended use is not permitted by statutory regulation or exceeds the permitted use, you will need to obtain permission directly from the copyright holder. To view a copy of this licence, visit <http://creativecommons.org/licenses/by/4.0/>.

References

1. C.C. Burt, Peripheral Skin Temperature In Normal Pregnancy. *The Lancet* **254**, 787–790 (1949). [https://doi.org/10.1016/S0140-6736\(49\)91371-9](https://doi.org/10.1016/S0140-6736(49)91371-9)
2. E. Dimitriadis, D.L. Rolnik, W. Zhou, G. Estrada-Gutierrez, K. Koga, R.P.V. Francisco, C. Whitehead, J. Hyett, F. da Silva Costa, K. Nicolaides et al., Pre-eclampsia. *Nat. Rev. Dis. Primers.* **9**, 8 (2023). <https://doi.org/10.1038/s41572-023-00417-6>
3. M. Costa, A.L. Goldberger, C.-K. Peng, Broken asymmetry of the human heartbeat: loss of time irreversibility in aging and disease. *Phys. Rev. Lett.* **95**, 198102 (2005). <https://doi.org/10.1103/PhysRevLett.95.198102>
4. C.K. Karmakar, A.H. Khandoker, J. Gubbi, M. Palaniswami, Defining asymmetry in heart rate variability signals using a Poincaré plot. *Physiol. Meas.* **30**, 1227 (2009). <https://doi.org/10.1088/0967-3334/30/11/007>
5. D. Zalas, W. Bobkowski, J. Piskorski, P. Guzik, Heart rate asymmetry in healthy children. *J. Clin. Med.* (2023). <https://doi.org/10.3390/jcm12031194>
6. R. Pawłowski, K. Buszko, J.L. Newton, S. Kujawski, P. Zalewski, Heart rate asymmetry analysis during head-up tilt test in healthy men. *Front. Physiol.* (2021). <https://doi.org/10.3389/fphys.2021.657902>
7. R. Pawłowski, P. Zalewski, J. Newton, A. Piątkowska, E. Koźluk, G. Opolski, K. Buszko, An assessment of heart rate and blood pressure asymmetry in the diagnosis of vasovagal syncope in females. *Front. Physiol.* (2023). <https://doi.org/10.3389/fphys.2022.1087837>
8. Z. Kreska, P. Mátrai, B. Nemeth, B. Ajtay, I. Kiss, L. Hejjel, Z. Ajtay, Physical vascular therapy (BEMER) affects heart rate asymmetry in patients with coronary heart disease. *In Vivo (Brooklyn)* **36**, 1408 (2022). <https://doi.org/10.21873/invivo.12845>
9. R.G. Ceballos-Juárez, E.Y. Pichardo-Carmona, H. Mendieta-Zerón, J.C. Echeverría, J.J. Reyes-Lagos, Multiscale asymmetry reveals changes in the maternal short-term heart rate dynamics of preeclamptic women during labor. *Technol. Health Care* **31**, 95–101 (2023). <https://doi.org/10.3233/THC-220042>
10. E.Y. Pichardo-Carmona, J.J. Reyes-Lagos, R.G. Ceballos-Juárez, C.I. Ledesma-Ramírez, H. Mendieta-Zerón, M.Á. Peña-Castillo, E. Nsugbe, M.Á. Porta-García, Y. Mina-Paz, Changes in the autonomic cardiorespiratory activity in parturient women with severe and moderate features of preeclampsia. *Front. Immunol.* (2023). <https://doi.org/10.3389/fimmu.2023.1190699>
11. A. Nicolò, C. Massaroni, E. Schena, M. Sacchetti, The importance of respiratory rate monitoring: from healthcare to sport and exercise. *Sensors (Switzerland)* **20**, 1–45 (2020)
12. K. Phan, S. Pamidi, Y.-H. Gomez, S.S. Daskalopoulou, Sleep-disordered breathing in high-risk pregnancies is associated with elevated arterial stiffness and increased risk for preeclampsia. *Am. J. Obstet. Gynecol.* **833**, e1-833.e20 (2022). (226–232)
13. D.L. Wilson, S.P. Walker, A.M. Fung, G. Pell, F.J. O'Donoghue, M. Barnes, M.E. Howard, Sleep-disordered breathing in hypertensive disorders of pregnancy: a BMI-matched study. *J. Sleep Res.* **27**, e12656 (2018). <https://doi.org/10.1111/jsr.12656>
14. R. Soni, M. Muniyandi, Breath rate variability: a novel measure to study the meditation effects. *Int J Yoga* **12**, 45 (2019). https://doi.org/10.4103/ijoy.ijoy_27_17
15. J. Piskorski, P. Guzik, The structure of heart rate asymmetry: deceleration and acceleration runs. *Physiol. Meas.* **32**, 1011 (2011). <https://doi.org/10.1088/0967-3334/32/8/002>
16. B. Biczuk, S. Buś, S. Żurek, J. Piskorski, P. Guzik, Statistical and diagnostic properties of PRR30, PRR3.25% and asymmetrical entropy descriptors in atrial fibrillation detection (2024)
17. L. Chladekova, B. Czipelova, Z. Turianikova, I. Tonhajzerova, A. Calkovska, M. Baumert, M. Javoroka, Multiscale time irreversibility of heart rate and blood pressure variability during orthostasis. *Physiol. Meas.* **33**, 1747 (2012). <https://doi.org/10.1088/0967-3334/33/10/1747>
18. ACOG, *Obstetrics & Gynecology* **133**, (2019)
19. M. Szmajda, M. Chyliński, J. Sacha, J. Mroczka, Three methods for determining respiratory waves from ECG (PART I). *Metrol. Meas. Syst.* **30**, 821–837 (2023). <https://doi.org/10.24425/mms.2023.147956>
20. N. Wessel, A. Voß, J. Kurths, P. Saparin, A. Witt, H.J. Kleiner, R. Dietz, Renormalised entropy: a new method of non-linear dynamics for the analysis of heart rate variability. *Comput. Cardiol.* **1994**, 137–140 (1994)

21. L.E.V. Silva, R. Fazan, J.A. Marin-Neto, PyBioS: a freeware computer software for analysis of cardiovascular signals. *Comput. Methods Programs Biomed.* **197**, 105718 (2020). <https://doi.org/10.1016/j.cmpb.2020.105718>
22. A. Porta, S. Guzzetti, N. Montano, T. Gneccchi-Ruscione, R. Furlan, A. Malliani, Time reversibility in short-term heart period variability; (2006), (ISBN 978-1-4244-2532-7)
23. P. Guzik, J. Piskorski, T. Krauze, A. Wykretowicz, H. Wysocki, Heart rate asymmetry by Poincaré plots of RR intervals. *Biomed Tech (Berl)* **51**, 272–275 (2006). <https://doi.org/10.1515/BMT.2006.054>
24. C. L. Ehlers, J. Havstad, D. Prichard, J. Theiler, Low doses of ethanol reduce evidence for nonlinear structure in brain activity (1998)
25. A. Porta, K.R. Casali, A.G. Casali, T. Gneccchi-Ruscione, E. Tobaldini, N. Montano, S. Lange, D. Geue, D. Cysarz, P. Van Leeuwen, Temporal asymmetries of short-term heart period variability are linked to autonomic regulation. *Am J Physiol-Regul Integr Comp Physiol* **295**, R550–R557 (2008). <https://doi.org/10.1152/ajpregu.00129.2008>
26. W. Chen, Z. Wang, H. Xie, W. Yu, Characterization of surface EMG signal based on fuzzy entropy. *IEEE Trans. Neural Syst. Rehabil. Eng.* **15**, 266–272 (2007). <https://doi.org/10.1109/TNSRE.2007.897025>
27. A.M.S. Borin, A. Humeau-Heurtier, L.E. Virgílio Silva, L.O. Murta, Multiscale entropy analysis of short signals: the robustness of fuzzy entropy-based variants compared to full-length long signals. *Entropy* (2021). <https://doi.org/10.3390/e23121620>
28. A.M.S. Borin, A. Humeau-Heurtier, L.E.V. Silva, L.O. Murta, Multiscale entropy analysis of short signals: the robustness of fuzzy entropy-based variants compared to full-length long signals. *Entropy* (2021). <https://doi.org/10.3390/e23121620>
29. A. Borin, A. Humeau-Heurtier, L. Virgílio Silva, L. Murta, L. Murta Multiscale Entropy Analysis, A. Monte Serrat Borin, L. Eduardo Virgílio Silva, L. Otávio Murta, The robustness of fuzzy entropy-based variants compared to full-length long signals. *Entropy* (2021). <https://doi.org/10.3390/e23121620>
30. M. Costa, J.A. Healey, Multiscale entropy analysis of complex heart rate dynamics: discrimination of age and heart failure effects. (2003)
31. M. Costa, A.L. Goldberger, C.K. Peng, Multiscale entropy analysis of complex physiologic time series. *Phys. Rev. Lett.* (2002). <https://doi.org/10.1103/PhysRevLett.89.068102>
32. G. Lancaster, D. Iatsenko, A. Pidde, V. Ticcinelli, A. Stefanovska, Surrogate data for hypothesis testing of physical systems. *Phys. Rep.* **748**, 1–60 (2018). <https://doi.org/10.1016/j.physrep.2018.06.001>
33. J. Theiler, S. Eubank, A. Longtin, B. Galdrikian, J. Doynne Farmer, Testing for nonlinearity in time series: the method of surrogate data. *Phys. D* **58**, 77–94 (1992). [https://doi.org/10.1016/0167-2789\(92\)90102-S](https://doi.org/10.1016/0167-2789(92)90102-S)
34. L.E.V. Silva, R.M. Lataro, J.A. Castania, C.A.A. Silva, H.C. Salgado, R. Fazan, A. Porta, Nonlinearities of heart rate variability in animal models of impaired cardiac control: contribution of different time scales. *J. Appl. Physiol.* **123**, 344–351 (2017). <https://doi.org/10.1152/jappphysiol.00059.2017>
35. K.J. Chang, K.M. Seow, K.H. Chen, Preeclampsia: recent advances in predicting, preventing, and managing the maternal and fetal life-threatening condition. *Int. J. Environ. Res. Public Health* **20**, 2994 (2023)
36. C. Karmakar, A. Khandoker, M. Palaniswami, Analysis of Slope based heart rate asymmetry using Poincaré plots. In: *Proceedings of the computing in cardiology*; Vol. 39 (2012)
37. D. Anderson, J. Mcneely, M. Chesney, B.G. Windham, Breathing variability at rest is positively associated with 24-h blood pressure level. *Am. J. Hypertens.* **21**, 1324–1329 (2008). <https://doi.org/10.1038/ajh.2008.292>
38. J.S. Gasior, J. Sacha, P.J. Jelen, J. Zielinski, J. Przybylski, Heart rate and respiratory rate influence on heart rate variability repeatability: effects of the correction for the prevailing heart rate. *Front. Physiol.* (2016). <https://doi.org/10.3389/fphys.2016.00356>
39. J. Mehlsen, K. Pagh, J.S. Nielsen, L. Sestoft, S.L. Nielsen, Heart rate response to breathing: dependency upon breathing pattern. *Clin. Physiol.* (1987). <https://doi.org/10.1111/j.1475-097X.1987.tb00153.x>
40. A. Pal, F. Martinez, M.A. Akey, R.S. Aysola, L.A. Henderson, A. Malhotra, P.M. Macey, Breathing rate variability in obstructive sleep apnea during wakefulness. *J. Clin. Sleep Med.* **18**, 825–833 (2022). <https://doi.org/10.5664/jcsm.9728>
41. Y.P. Wang, T.B.J. Kuo, G.Z. Wang, C.C.H. Yang, Different effects of inspiratory duration and expiratory duration on heart rate deceleration capacity and heart rate asymmetry. *Eur. J. Appl. Physiol.* (2024). <https://doi.org/10.1007/s00421-024-05433-2>
42. O.F.C. van den Bosch, R. Alvarez-Jimenez, H.-J. de Grooth, A.R.J. Girbes, S.A. Loer, Breathing Variability—Implications for Anaesthesiology and Intensive Care. *Crit. Care* **25**, 280 (2021). <https://doi.org/10.1186/s13054-021-03716-0>